

## 77 GHz MICROSTRIP ANTENNA WITH GAP COUPLED ELEMENTS FOR IMPEDANCE MATCHING

F. D. L. Peters, S. O. Tatu, and T. A. Denidni

INRS-EMT

University of Québec, Place Bonaventure  
800, de la Gauchetière Ouest, suite 6900  
Montréal (Québec) H5A 1K6, Canada

**Abstract**—This work focuses on microstrip patch antennas for the 77 GHz millimeter band. For some combinations of the parameters *microstrip width*, *free wavelength* and substrate *permittivity*, impedance matching via inset fed is found to be non applicable. The current distribution of the desired  $TM_{10}$  mode is partially disturbed. Gap coupled parasitic microstrips are analyzed in order to match the feeding impedance to the feeding microstrip while improving the bandwidth in these particular cases.

### 1. INTRODUCTION AND MOTIVATION

Generally discussed in [1] and [2], the return loss of a mismatched microstrip fed antenna can be decreased significantly by an accompanying gap coupled microstrip element. This work analyzes if the gap coupled technique may serve in those cases where the inset fed method leads to a very low gain patch.

This project employs a substrate thickness of 5 mil, i.e., 0.127 mm with a relative permittivity of  $\varepsilon = 9.9$  as well as the commercial software *Momentum*. It focuses on a patch antenna connected to a  $50\ \Omega$  feeding microstrip of width  $w = 5$  mil. Subsequently the results are compared to a  $33\ \Omega$  equivalent, i.e.,  $w = 10$  mil.

Lots of existing methods applying slots in order to improve the performance of a single layer microstrip antenna provide motivation for this work. It is most important to have a uniform current distribution before disturbing it intentionally. Approaches like U-slots

---

Corresponding author: F. D. L. Peters (peters@emt.inrs.ca).

or rectangular slots as discussed in [3–5] take an undisturbed  $TM_{10}$  or higher as an essential starting point.

**Gap coupling** for lower frequency bands is summarized e.g., in [6, 7] which describe mostly probe fed constellations. Exciting multiple different resonance frequencies — at least two — lead to broader impedance bandwidth and improved gain when losses are low. However, precise general design procedures are not given due to the complex behaviour of the parameters.

Subsequently to the analysis in Section 2, the basic design and design procedure can be found in Sections 3 and 4. Results for the variation in radiation pattern, gain and efficiency are discussed in Section 5.

## 2. ANALYSIS

### 2.1. Current Distribution

A common way to feed rectangular microstrip patch antennas (RMSA) is to connect a coaxial probe on the level of half the width of the RMSA, i.e.,  $y = W_{\text{PATCH}}/2$ . Moving the probe from the edge towards the center along the  $x$ -axis decreases the input impedance.

This way ensures to excite only those modes which produce the desired radiating edges (fringing slots).  $TM_{10}$  is mostly responsible for a linear polarization and radiation defining the  $E$ -plane, but higher order modes can be excited and used in order to perform broadband radiation, e.g., shown in [4].

In millimeter bands probes cannot be applied to a patch. However, simulation of the ideal probe excitation (with a zero reactance probe) yields a wide zone in which an almost perfect sinusoidal distribution is observed, see Figure 1.

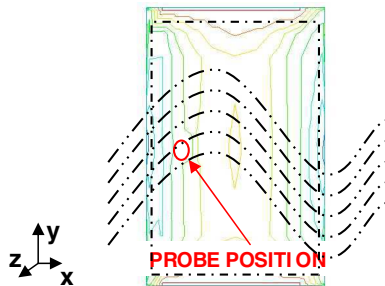


**Figure 1.** Ideal current distribution of a probe excited patch.

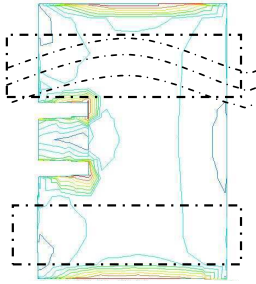


**Figure 2.** Reduced zones of undisturbed current distribution.

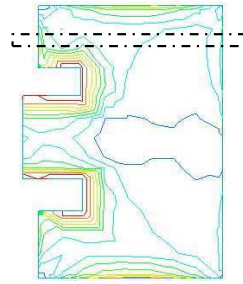


**Figure 3.** Virtually vanished undisturbed  $TM_{01}$  regions.

Since moving the probe, i.e., the position of excitation, is not applicable, the microstrip *inset fed technique* serves instead for the same purpose.

Similar to the probe, in case of a sinusoidal current distribution along the  $x$ -axis, the input impedance decreases towards the center. Figure 2 depicts the undisturbed zones, (enclosed by a dotted rectangular) of sinusoidal distribution.

The inset fed formulas containing a  $\cos^2$ -dependency

$$R_{EDGE} = 90 \frac{e_r^2}{e_r - 1} \left( \frac{L_{PATCH}}{W_{PATCH}} \right)^2 W \quad (1)$$

$$R_{inset} = R_{EDGE} \cos(\pi \times L_{PATCH})^2 \quad (2)$$

were derived based on observations with coaxial probes. The particular effect of the microstrip was not taken into account until recently [8–10] discussed these differences especially for the inset fed method.

Equation (2) fails with a feeding line of twice the width relative to the previous example of Figure 2. Despite the fact that the entire surface has not decreased significantly compared to Figure 2, the main mode along the  $x$ -axis can virtually no longer be observed in Figure 3 due to the proximity of the inset fed to the non radiating edge. Hence, impedance has to be matched in an alternative way.

### 3. DESIGN AND SIMULATION

#### 3.1. Basic Patch Design

The RMSA is designed to carry a  $TM_{10}$  mode and to provide linear polarized broadside radiation. The length of the patch ( $L_{PATCH}$ ) is chosen to be  $\lambda_{eff}/2$ . Generally, the resonance frequency of a

rectangular patch can be calculated via the (desired) excited mode  $TM_{nm}$  by

$$f_{res} = \frac{c}{2\sqrt{\varepsilon_{eff}}} \sqrt{\left(\frac{m}{L}\right)^2 + \left(\frac{n}{W_{PATCH}}\right)^2}. \quad (3)$$

Furthermore the width of the patch  $W_{PATCH}$  can be designed based on the following formula

$$W_{PATCH} = \frac{c}{2f_0} \sqrt{\frac{2}{\varepsilon_r + 1}}. \quad (4)$$

In case of 77 GHz,  $\varepsilon = 9.9$  and  $h = 0.127$  mm the resulting  $W_{PATCH} = 0.828$  mm is about 1.5 times the length  $L_{PATCH}$  and only 6.5 times  $W_{STRIP}$ , the width of the feeding microstrip. Any quotient of  $W_{STRIP}/W_{PATCH} < 5$ , obliged by application, size requirements, etc., leads to unpredictable results.

### 3.2. Parasitic Microstrip Patches

The proposed idea contains a main basic patch (3.1) gap coupled to 7 individual microstrips of equal length ( $L_{PAR}$ ), see Figure 10. Both RMSA and parasitic microstrips provide real impedance at resonance when observed independently. Brought together, the second parasitic resonance circuit is transformed into the input impedance.

**Table 1.** Length and width of two considered patches.

Nr#	$L_{PATCH}/\text{mm}$	$L_{PAR}/\text{mm}$	$W_{PATCH}/\text{mm}$	Gap $d$ (average)
#1	0.547	0.52	0.828	0.138 mm
#2	0.5739	no	0.8498	no

## 4. DESIGN PROCEDURE

The design procedure of the impedance matching and bandwidth enhancing method can be summarized in the following sub steps:

- Choice of the default lengths  $L_{PATCH}$  and  $L_{PAR}$
- Choice of average gap distance
- Placing *head of the loop* onto the center frequency (CF)
- Adjusting the loop size

It is obvious that the length of both the patch and the small parasitic strips are independently defining the eigenfrequency. In a first step both eigenfrequencies are chosen to be rather close to the desired CF, i.e., within 0.5–1% of the CF. The main patch should be closer to the CF. Figure 4 shows in dotted lines both resonances before coupling. In resonance the real part of the impedance becomes maximal.

Once gap coupled together, two impedance loci peaks can be detected in the reactive part. The right one still represents the parasitic patches.

The smaller is the gap the lower is the frequency of the *loop head* of the impedance coupling loop in the smith chart. Choosing the gap distance should roughly set the head of loop frequency equal to the desired CF; the behaviour is shown in Figure 5. The main patch length

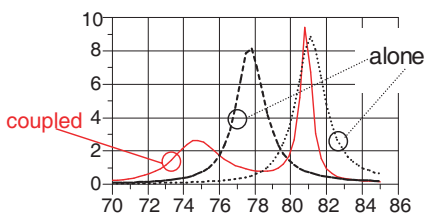


**Figure 4.** Real part of impedance shows two maxima caused by two eigen-resonance frequencies.

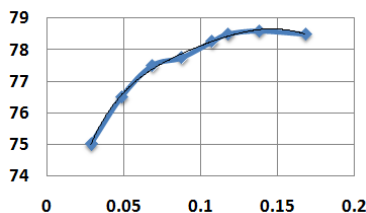


**Figure 5.** Loop head frequency as a function of the average distance  $d$ .

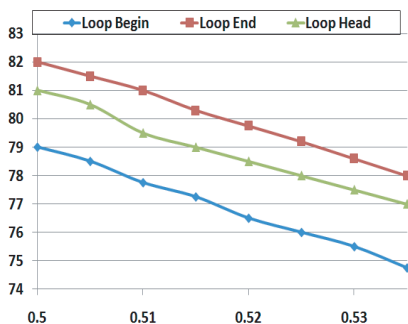


**Figure 6.** Lin. behaviour between  $L_{PAR}$  (mm) and the impedance loop frequencies, (const.  $L_{PATCH}$  and  $d$ ).

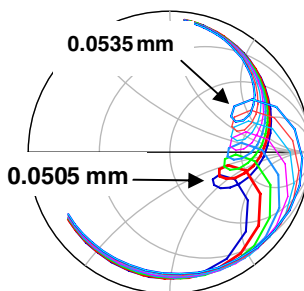


**Figure 7.** Additionally to Figure 6, the loop varies in phase as a function of  $L_{PAR}$ .

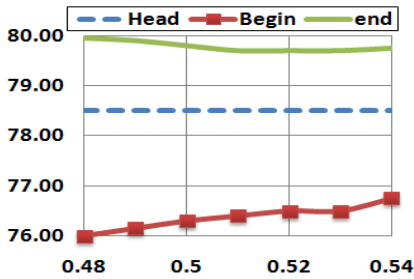


**Figure 8.**  $X$ -axis =  $L_{PATCH}$ ,  $L_{PAR}$  is kept constant.

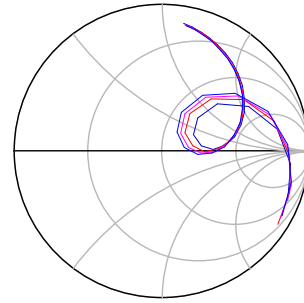


**Figure 9.** Due to the small narrow slots the “oupling loop” can be modified accurately.

should be chosen in a way that the desired CF is approximately located in the middle between the steep and flat section.

Next, Figure 6 depicts three defined loop frequencies as a function of the parasitic microstrip length ( $L_{PAR}$ ). Figure 7 displays the same in the Smith chart. The main patch is kept constant, and the gap distance  $d$  is readjusted each time to  $d = 0.1378$  mm.

The interval of  $L_{PAR}$  is chosen in a way that the *loop head* frequency moves towards the desired CF. The linear behaviour allows to place the loop head onto the CF by modifying the parasitic strip length ( $L_{PAR}$ ).

Additionally in Figure 8 it can be seen that readjusting the main patch length slightly modifies the loop size which is equivalent to the bandwidth, but keeps the *loop head* frequency constant.

By manually increasing or decreasing the individual gap between the strip and the main patch, the loop size can be modified very precisely, see the example in Figure 9. The result is a loop head frequency in the center of the Smith chart. Readjust the steps if the loop is much below the real axis. Be sure to obtain a phase a little bit above the real axis before increasing the size.

## 5. RESULTS

This section depicts the currents, return loss, bandwidth and some radiation characteristics of the analyzed idea.

### 5.1. Current Distribution

Referring to Subsection 2.1, one major aim is to excite only those modes which exhibit a half wavelength variation (or multiples) along  $x$ -axis, preferable  $TM_{10}$  in the present case. As Figure 10 displays with a 5 mil feeding, a homogenous field along the radiating ( $y$ -axis) edges is obtained, but with some exceptions due to the microstrip.

### 5.2. Scattering Parameters

The comparison between the inset fed patch and a couple of gap coupled equivalents is shown in Figure 11. As depicted, every constellation is very well matched at the desired CF of 77 GHz.  $S_{11}$  of the gap coupled antenna can be easily brought to  $-45$  dB by slightly modifying the gap distance of only one microstrip. The optimized gap coupled patch shows a broader relative bandwidth of about 2.5 times initial value.

Figure 12 in  $Z$ -plane exhibits the typical coupling loop. Head and end of the loop lie on the real axis. This constellation yields almost the best achievable bandwidth while maintaining minimal return loss.

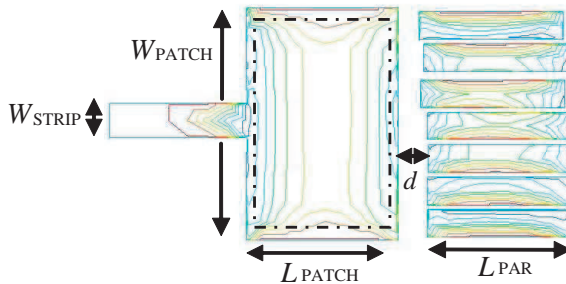


**Figure 10.** Homogenous field along  $y$ -axis in a wide zone,  $\lambda/2$  variation over  $x$ -axis.

### 5.3. Feeding with a Double Sized $W_{PATCH}$

In the following, a conventional inset fed patch with 5, resp. 10 mil = 0.254 mm, (Figure 3), is compared to the gap coupled equivalents. As discussed previously, no matching can be achieved with inset and 10 mil. In contrast, with gap coupling it can be shown that the disturbance introduced by the microstrip at  $x = 0$  is slightly bigger, see Figure 13. Despite this effect, the bandwidth and matching are very

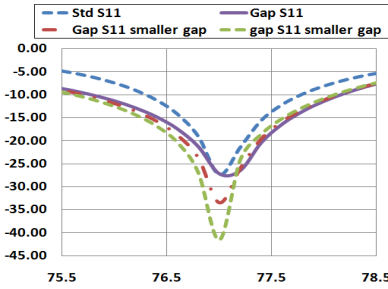


**Figure 11.**  $S_{11}$  of the inset fed antenna compared to the gap coupled one with 3 different gap distances.

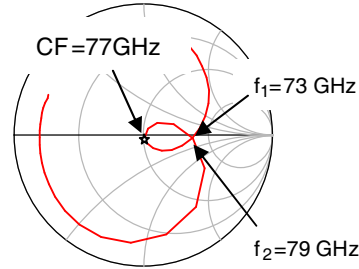


**Figure 12.** Impedance loop, perfectly placed.

good, see Figure 14. Radiation in  $E$ -Plane remains almost identical, see Figure 18.

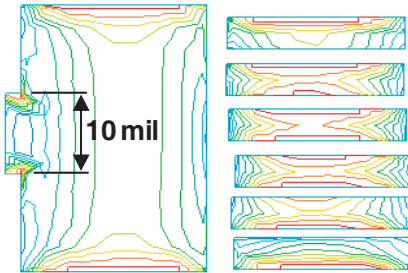


**Figure 13.** Feeding line with 10 mil = 0.254 mm and  $TM_{10}$  distrib.

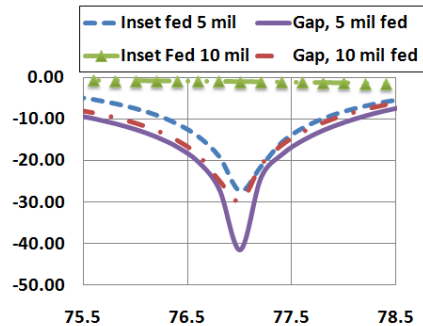


**Figure 14.**  $S_{11}$  inset fed, resp. gap coupled antenna with 5 mil 10 mil feeding.

### 5.4. Radiation Pattern

The radiation pattern of the coupled patches yields a shift to the right in  $E$ -plane, see Figure 16, compared to the inset fed in Figure 15, responsible for an unavoidable small phase shift on the second patch. The angle of the shift in radiation is almost independent from frequency



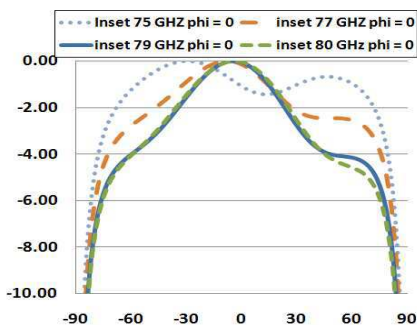


**Figure 15.** Radiation i. *E*-Plane, inset fed.

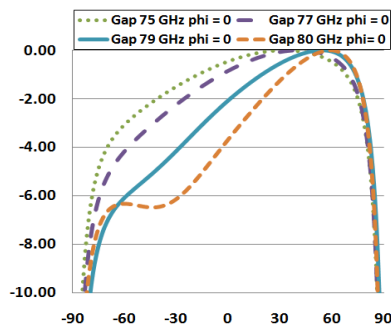


**Figure 16.** Radiation pattern in *E*-Plane, gap coupled.

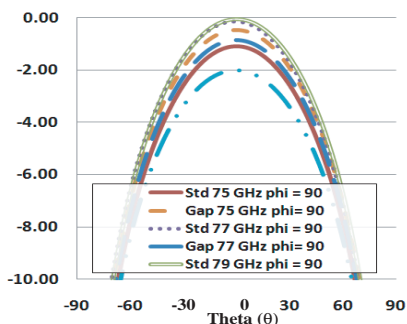


**Figure 17.** Comparison of all constellations and frequencies in *H*-plane.

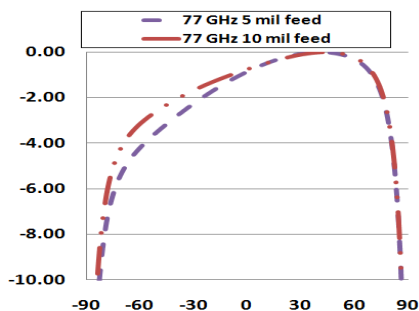


**Figure 18.** Radiation pattern gap coupled, 5 and 10 mil feeding strips.

within a band of  $> 5\%$ , but becomes more considerable when the frequency turns towards the eigenfrequency of the parasitic elements. Future work will analyze if additional opposed elements reduce the tilt.

Gain is little affected in *E*-plane (though shifted in  $\theta$ ) by the introduced losses in the parasitic elements. Comparing the 5 mil inset fed with the gap coupled solution, a delta of about 0.5 dB is observed. The peak gain in *E*-plane is 10.2/10.7 dB for gap/inset and 10.4/8.6 dB in *H*-plane, i.e., about 2 dB loss in the latter case.

The total radiated power is virtually identical. The inset itself causes losses in the conventional solution, which equals approximately the parasitic microstrip losses.

The effect on cross polarization is depicted in Figure 19. The parasitic microstrips introduce cross polarized radiation considered

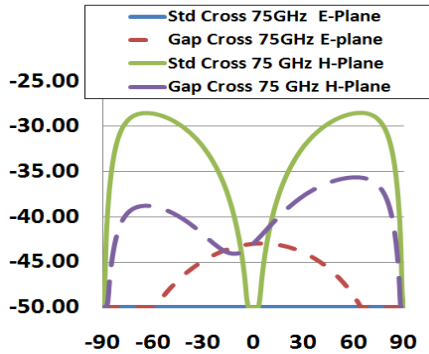


**Figure 19.** Cross polarization in  $H$ -plane and in  $E$ -plane.

from  $E$ -plane. On the other hand, in  $H$ -plane less cross polarization is observed than with the inset fed.

## 6. CONCLUSION

In this work, limitations of the inset fed method have been outlined. A simple but efficient idea for particular configurations is presented and implemented, which allows to increase the bandwidth and match the feeding microstrip. The design procedure allows to graphically adjust the coupling loop to the desired CF. Degradations in the radiation pattern are small. While the gain decreases slightly, bandwidth increases, and the current distribution on the main patch shows a  $TM_{10}$  mode.

## REFERENCES

1. Song, Q. and X.-X. Zhang, "A study on wideband gap-coupled microstrip antenna arrays," *IEEE Transactions on Antennas and Propagation*, Vol. 43, No. 3, 313–317, 1995.
2. Lee, C. S. and V. Nalbandian, "Impedance matching of a dual-frequency microstrip antenna with an air gap," *IEEE Transactions on Antennas and Propagation*, Vol. 41, No. 5, 680–682, 1993.
3. Sze, J.-Y. and K.-L. Wong, "Slotted rectangular microstrip antenna for bandwidth enhancement," *IEEE Transactions on Antennas and Propagation*, Vol. 48, No. 8, 1149–1152, 2000.
4. Maci, S., G. B. Gentili, P. Piazzesi, and C. Salvador, "Dual-band slot-loaded patch antenna," *IEE Proceedings — Microwaves, Antennas and Propagation*, Vol. 142, No. 3, 225–232, 1995.

5. Chai, W.-W., X.-J. Zhang, and S.-G. Liu, "Wideband microstrip antenna array using U-slot," *PIERS Online*, Vol. 3, No. 7, 1085–1088, 2007.
6. Kumar, G., *Broadband Microstrip Antennas*, Artech House, Boston Mass. U. A., 2003.
7. Ray, K. P., S. Ghosh, and K. Nirmala, "Compact broadband gap-coupled microstrip antennas," *IEEE Antennas and Propagation Society International Symposium 2006*, No. 9–14, 3719–3722, 2006.
8. Ramesh, M. and YIP KB, "Design formula for inset fed microstrip patch antenna," *Journal of Microwaves and Optoelectronics*, Vol. 3, No. 6, 5–10, 2003.
9. Basilio, L. I., M. A. Khayat, J. T. Williams, et al., "The dependence of the input impedance on feed position of probe and microstrip line-fed patch antennas," *IEEE Transactions on Antennas and Propagation*, Vol. 49, No. 1, 45–47, 2001.
10. Hu, Y., D. R. Jackson, J. T. Williams, S. A. Long, and K. V. Rajan, "Characterization of the input impedance of the inset-fed rectangular microstrip antenna," *IEEE Transactions on Antennas and Propagation*, Vol. 56, No. 10, 3314–3318, 2008.